ELSEVIER

Lithos 52 (2000) 235–252

LITHOS

www.elsevier.nl/locate/lithos

Petrotectonic evolution of the high- to ultrahigh-pressure Maksyutov Complex, Karayanova area, south Ural Mountains: structural and oxygen isotope constraints

Mary L. Leech *, W.G. Ernst

Geological and Environmental Sciences, Stanford University, Stanford, CA 94305-2115, USA

Abstract

The Maksyutov Complex consists of three fault-bounded lithologic units: a quartzofeldspathic gneiss containing mafic eclogite boudins (Unit #1); a metasedimentary blueschist-facies (Yumaguzinskaya) unit; and a meta-ophiolitic mélange (Unit #2). The geologic history of the high- to ultrahigh-pressure (HP–UHP) assembly of the Maksyutov Complex is complicated by several stages of prolonged retrograde metamorphism and deformation. The Sakmara River exposes all three units near the former village of Karayanova. A structural/petrologic cross-section through the area yields new quantitative data for the complex and, regionally, for the south Urals. Analysis of the Karayanova area has identified the major structures. Regional folding within the complex is parallel to the dominant foliation trending northeast–southwest. Stereonet data show that, during exhumation, this large-scale folding was refolded about axes trending southeast. Unit #1 and the Yumaguzinskaya are tectonically and petrologically distinct units juxtaposed by west-vergent thrusting and recrystallization within the same subduction zone. A shear zone developed later between Unit #2 and the Unit #1 + Yumaguzinskaya tectonic package accompanying exhumation. Field relations and petrofabric demonstrate that blueschist-facies recrystallization overprinted an earlier eclogite-facies metamorphism. Thermobarometric measurements yield P–T values of 594–637°C, 1.5–1.7 GPa for eclogite, but these conditions may reflect annealing during the early-stage exhumation at ~375 Ma. Cuboid graphite aggregates testify to precursor conditions for Unit #1 within the diamond stability field, if such textures are correctly interpreted. Measured $^{18}O/^{16}O$ partitioning between pairs of coexisting phases yield three main recrystallization temperature ranges: (1) 678 ± 83°C, attending Unit #1 eclogite-facies metamorphism; (2) 453 ± 17°C, during transitional blueschist/greenschist-facies metamorphism for the amalgamated Unit #1 + Yumaguzinskaya + Unit #2 assembly; and (3) 250 ± 68°C, reflecting late-stage hydrothermal alteration and exhumation. Oxygen isotope data for Units #1 and #2 indicate that garnet, blue amphibole, and pyroxene crystallized in isotopic equilibrium, validating previous thermobarometric calculations for a Unit #1 retrograde metamorphic event. Variations in $\delta^{18}O$ values for phengites suggest the possibility of late metamorphic fluid infiltration. Retrograde recrystallization at high pressure in the presence of fluids and a calculated

* Corresponding author. Department of Geology, University of London, Royal Holloway, Egham, Surrey TW20 0EX, UK. Fax: +44-01784-471-780; e-mail: m.leech@gl.rhbnc.ac.uk, mary@geo.stanford.edu

PII: S0024-4937(99)00093-6

slow exhumation rate for the Maksyutov Complex account for the fact that inferred UHP coesite and diamond were completely back-reacted during decompression.

Keywords: Maksyutov Complex; Ural Mountains; High- to ultrahigh-pressure; Oxygen isotopes; Structural geology; Tectonic evolution

1. Introduction

Most reports on the Maksyutov subduction complex focus on the petrology of the high- to ultrahigh-pressure (HP–UHP) eclogitic unit; this is the lithology from which the first descriptions of possible pseudomorphs after coesite were reported by Chesnokov and Popov (1965). Until recently, little was known about the overall structure and deformational history of the complex and its relationship to an exhumation mechanism. In this paper, we present new petrological, geochemical, and structural components of the Maksyutov Complex in order to develop an overall model for its petrotectonic development. A complete cross-section through the Maksyutov Complex is exposed along the Sakmara River near Karayanova showing the structural relationships among all three units and exposing most rock types in a relatively small area (Fig. 1). Previously, the only study incorporating significant structural data for the complex concentrated on a transect through Antingan, an area lacking extensive exposure, several kilometers southeast of the Karayanova area (Hetzel et al., 1998). We focus on eclogitic Unit #1 which preserves several stages in the history of the Maksyutov Complex since the HP–UHP metamorphism.

Leech and Ernst (1998) investigated graphite cuboids from metapelites which may represent pseudomorphs after diamond, thus, suggesting the possibility of UHP metamorphism for Unit #1; although still problematic, we will refer to the highest pressure metamorphic event as the UHP event. Most likely, slow exhumation relative to other UHP terranes and the influx of aqueous fluids caused UHP index phases to re-equilibrate under lower P–T conditions, explaining the lack of relict coesite or diamond in the Maksyutov Complex (Hacker and Peacock, 1995; Ernst et al., 1997; Webb et al., 1999). Preservation of diamond relics, chiefly as armored micro-inclusions in garnet and zircon which act as pressure vessels, requires an exhumation rate so rapid that the diamond-bearing rocks did not reside at depth long enough to re-equilibrate to graphite (Sobolev and Shatsky, 1990; Sobolev et al., 1994).

2. Geologic setting

2.1. Development of the Ural Mountains

The Urals are an approximately 2300-km long, 400-km wide orogen formed by oblique collision between the East European platform and microcontinental and cratonal blocks on the east during the Late Paleozoic (Zonenshain et al., 1984, 1990; Lennykh et al., 1995; Dobretsov et al., 1996; Puchkov, 1997). The Uralian collision began in the south in the Late Devonian, possibly pivoting on an East European platform promontory in the central Urals, and finally reaching full-collision in the polar Urals by the Late Permian. The major suture of the Urals is the ophiolitic Main Uralian Fault (MUF); rocks to the west have protolith affinities with the East European platform and form the HP and UHP subduction belt, whereas rocks to the east are low-grade, greenschist-facies island arc complexes that developed on the hanging-wall plate.

The Maksyutov Complex extends more than 120 km north–south in the south Urals in the footwall of the MUF. Part of the leading edge of the East European platform was subducted beneath the Magnitogorsk island arc complex supplying the sedimentary protolith to the Maksyutov Complex. An early phase of extension, preserved as a series of deep, extensional basins beneath the Uralian foreland, along the eastern margin of the East European platform likely resulted in the shallow intrusion of mafic sills or dikes within the sedimentary section (Puchkov,

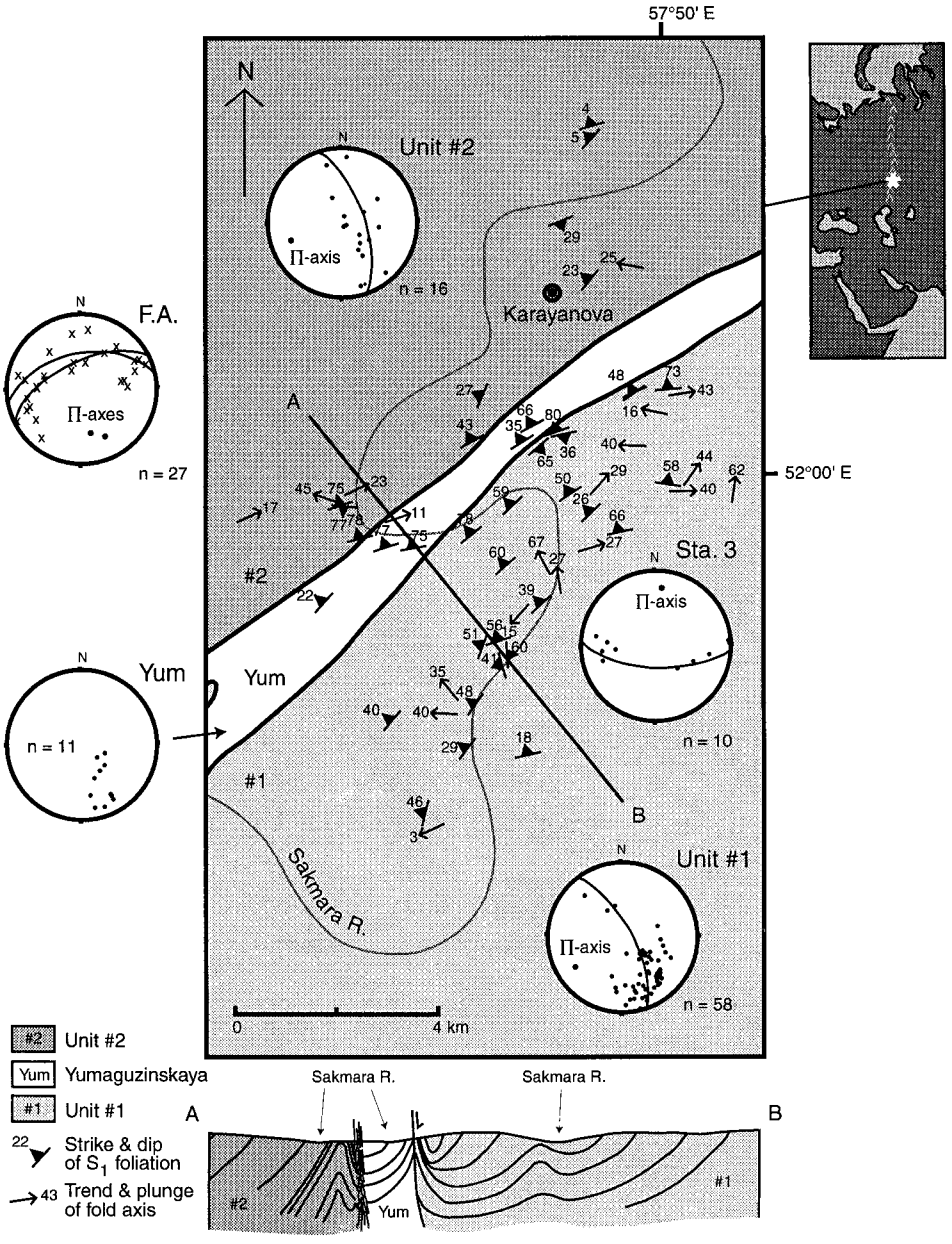

Fig. 1. Simplified geologic map of the Karayanova area with structural data superimposed. The cross-section shows the large-scale relationship between units (no vertical exaggeration). Equal area stereonets showing structural data for the Karayanova area including: (Unit #1) poles to foliation in Unit #1 with a π-axis (pole to the great circle) showing trend of southwest-trending folding; (Station 3) poles to foliation and a π-axis to small-scale folding at our Station 3 varying no more than 20° from Units #1 and #2 data; (Yum) poles to foliation for the Yumaguzinskaya unit; (Unit #2) poles to foliation and π-axis in Unit #2; and (F.A.) fold axes for Units #1 and #2 and their corresponding π-axes for the later south–southeast-trending folding event.

1997; Diaconescu et al., 1998; Brown and Spadea, 1999); these mafic intrusions probably constitute the basaltic protoliths for eclogite in the Maksyutov Complex. For a detailed examination of the sur-

rounding geology of the mountain belt, see Brown et al. (1996).

2.2. Overview of the Maksyutov Complex

The Maksyutov Complex consists of three main fault-bounded units: an eclogite-bearing gneiss, Unit #1; the intermediate metamorphic grade metasedimentary Yumaguzinskaya unit; and a meta-ophiolite mélange, Unit #2 (Fig. 1). Unit #1 contains boudins of eclogite, layers of eclogitic gneiss, and very rare ultramafic bodies within host metasedimentary garnet gneiss, mica schist, and quartzite. The Yumaguzinskaya contains rock types similar to Unit #1, but has been metamorphosed to no more than lower blueschist-facies and lacks mafic rocks; it apparently represents a higher crustal level than that of Unit #1. Unit #2 consists of lenses of serpentinite mélange and blocks of metasomatic rock (~ rodingite), metabasalt, and Ordovician/Silurian marble within mica schist and graphitic quartzite host rocks (Dobretsov et al., 1996); peak metamorphism for Unit #2 was transitional greenschist–blueschist-facies. Unit #2 and the Yumaguzinskaya, considered to tectonically overlie Unit #1 (Lennykh et al., 1995; Hetzel et al., 1998), were juxtaposed with Unit #1 in the subduction zone after the Early to Middle Devonian UHP metamorphic event that affected only Unit #1 (Matte et al., 1993; Beane, 1997; Beane et al., 1995). All three units subsequently were overprinted by a late, low-pressure greenschist-facies metamorphism and folded together about NE–SW trending axes.

Fe–Mg exchange geothermometry calculated for garnet and clinopyroxene (Powell, 1985) yields an equilibrium temperature ranging from 594°C to 637°C for eclogites from Unit #1. Minimum pressure estimates using the jadeite component of clinopyroxene (Holland, 1980) range from 1.5 to 1.7 GPa (Beane et al., 1995; Hetzel et al., 1998; Leech and Stockli, in press), but could be as high as 3.1 GPa if the graphite aggregates described by Leech and Ernst (1998) are, in fact, pseudomorphs after diamond. It is also possible that these thermobarometric values may represent annealing during exhumation whereby minerals re-equilibrated under lower P–T conditions, leaving little evidence of an earlier UHP metamorphism.

2.3. Occurrence and ages of HP to UHP metamorphic rocks

Attempts at a well-constrained age for the highest-pressure metamorphic stage for the Unit #1 eclogites have so far been inconclusive (Leech and Stockli, in press). Rutiles dated using conventional U–Pb TIMS methods give ages ranging from 377 ± 2 to 384 ± 4 Ma (Beane, 1997); however, the closure temperature for rutile in this chemical system is not well known, and estimates range from 380°C to 650°C (Mezger et al., 1989; Zalduegui et al., 1996). Preliminary Sm–Nd dating of garnet and pyroxene has yielded widely varying dates ranging from 357 $\pm$ 15 to 404 ± 20 Ma (Shatsky et al., 1997; Beane, unpublished data); the mineral separates investigated by Shatsky et al. probably contained inclusions, because they described eclogite samples with abundant atoll garnets. These Sm–Nd data overlap considerably with geochronologic results for lower temperature isotopic systems; this apparent age range could, in part, be explained by mixing between the porphyroblastic garnet and inclusions. Because dated basaltic rocks from other areas in the south Urals that are likely analogues to the eclogitic protolith in the Maksyutov Complex yield ages near 400 Ma, UHP metamorphism probably occurred between 400 and 375 Ma, but until more definitive data become available, it is impossible to date the UHP event exactly.

2.4. Constraints on exhumation and late-stage evolution

Intermediate-temperature $^{40}Ar/^{39}Ar$ data from Unit #1 phengite yield ages from 372 ± 3 to 377 ± 3 Ma (Beane, 1997), reflecting equilibration during an early stage in the exhumation history. $^{40}Ar/^{39}Ar$ analyses for the Yumaguzinskaya unit provide ages from 356 ± 3 to 365 ± 2 Ma; in contrast, Unit #2 rocks range from about 332 ± 3 to 339 ± 3 Ma. Apatite fission-track modelling results obtained by Leech and Stockli (in press) indicate that the Maksyutov Complex was exhumed to upper crustal levels and cooled below 110°C en masse during the Late Carboniferous (~ 315 Ma). An east–west transect at Karayanova shows that significant inter-unit movement in the Maksyutov Complex ceased after

about 315 Ma. The range of $^{40}Ar/^{39}Ar$ ages, combined with apatite fission-track data, indicates that the three units were juxtaposed between about 330 and 315 Ma.

3. Field relations and petrography

Field relations and metamorphic/deformational fabrics for thin sections from Unit #1 in the Karayanova area are summarized below in order to describe the multistage evolution of the Maksyutov Complex. Table 1 lists the mineral assemblages that document various stages of metamorphic mineral growth for the different rock types; abbreviations used are after Kretz (1983) except for phengite which we have abbreviated here as Phn. Petrography and microstructures from all three Maksyutov units have been described in detail by other workers (Beane, 1997; Beane et al., 1995; Lennykh et al., 1995; Hetzel et al., 1998). For brevity, we describe only field relations and sample descriptions relevant to the metamorphic and structural evolution of the complex, concentrating on Unit #1 because the history of this lithotectonic unit tracks the longest-term development.

3.1. Bulk-rock chemistry

Eleven samples were chosen for bulk-rock chemical analysis. Standard XRF techniques were employed by XRAL analytical laboratories. The results, listed in Table 2, provide a rough indication of the range of Maksyutov lithologies subjected to HP–UHP metamorphism; bulk-rock compositions compare reasonably well with those of other subduction-zone complexes. Aspects of the chemical range of the newly analyzed specimens are illustrated in Fig. 2. The six analyzed eclogites and two blueschists exhibit broad compositional overlap, suggesting that only minor metasomatic exchange between different lithologies accompanied the multistage recrystallization. Relatively modest amounts of titanium, total iron, and P_2O_5 indicate MORB-type affinities for the mafic units (Wilson, 1989). Alkalis, TiO_2, and P_2O_5 contents are directly proportional, and Cr_2O_3 and MgO contents are inversely proportional to Fe_2O_3 (total) and SiO_2, reflecting fractionation of the parental basalt magma. For some components, the quartzofeldspathic garnet gneisses appear to lie on the same chemographic trend lines as the mafic suite, but contrast with the eclogites and blueschists in being relatively K- and Zr-rich, Ca-, Na-, and Ti-poor.

3.2. Eclogite mineral chemistry

Mafic eclogite occurs throughout Unit #1 of the Maksyutov Complex as large tectonic blocks up to tens of meters in length, eclogitic gneissic bands transposed parallel to compositional layering, and boudins (10 cm to 2 m in length) within host phengite schists, garnet gneisses, and quartzites. Schists

Table 1
Mineral assemblages for Unit #1 samples showing UHP and retrograde mineralogy

Sample no.	Location	Rock type	Peak metamorphic mineralogy	Retrograde mineralogy
M-16	Karayanova	Mica schist	Phn + Qtz + Ab + Grt + Rt + Cal + Zrn + Pl	Phn + Qtz
MC-37	Karayanova	Eclogitic gneiss	Grt + Cpx + Phn + Qtz + Rt	Gln + Phn + Qtz + Pl + Chl
MC-38	Karayanova	Eclogitic gneiss	Grt + Cpx + Phn + Zrn + Ap	Gln + Lws + Phn + Pl + Qtz + Chl
MC-98	Karayanova	Eclogite	Grt + Cpx + Phn + Zrn + Ap	Phn + Qtz + Ab + Rt
MC-109	Karayanova	Eclogite w/Lws	Grt + Cpx + Phn + Qtz + Rt	Gln + Lws + Qtz + Chl
MC-116	Antingan	Eclogitic gneiss	Grt + Cpx + Phn + Ap	Grt + Lws + Phn + Qtz + Ep
MC-118	Antingan	Eclogite	Grt + Cpx + Zrn + Ap	Grt + Phn + Qtz
MC-154	Shubino	Eclogite	Grt + Cpx + Phn + Rt + Zrn + Ap	Phn + Chl + Qtz
MC-156	Shubino	Eclogite	Grt + Cpx + Phn + Gln + Rt	Phn + Qtz
MC-161	Shubino	Eclogite	Grt + Cpx + Phn + Zo + Pl + Mag + Rt + Zr + Ap	Gln + Phn + Qtz
MC-178	Karayanova	Eclogite	Grt + Cpx + Phn + Rt + Ap + Zr	Gln + Lws + Ab + Qtz

Table 2
Representative X-ray fluorescence data for Unit #1 eclogite and host gneisses from Karayanova; MC-204 from Antingan

Sample no.	UM-35d	UM-2a	UM-5	UM-13j	UM-10	MC-98	MC-99	MC-180	MC-156	MC-182	MC-204
Rock type	Eclogite	Quartzite	Eclogite	Blueschist	Grt gneiss	Eclogite	Eclogite	Blueschist	Eclogite	Grt gneiss	Eclogite
SiO_2 (wt.%)	40.60	91.80	49.0	43.20	54.00	49.80	50.40	47.60	48.80	61.50	47.90
TiO_2	2.70	0.17	1.52	0.71	1.22	0.94	1.52	1.61	3.12	1.04	1.93
Al_2O_3	16.30	3.82	14.2	16.90	16.00	13.90	13.90	16.60	12.70	16.10	13.60
Fe_2O_3 (total)	19.40	1.54	13.8	10.60	11.60	11.00	13.20	12.30	14.30	8.33	15.10
MnO	0.34	0.05	0.22	0.23	0.20	0.25	0.20	0.16	0.21	0.16	0.19
MgO	5.15	0.61	6.63	10.90	3.27	6.49	6.60	5.85	7.12	4.06	7.64
CaO	10.50	0.24	8.78	7.74	7.07	8.48	8.07	9.44	8.63	2.25	7.18
Na_2O	1.33	0.08	4.72	2.49	3.19	4.93	4.77	2.93	2.85	0.44	3.47
K_2O	0.07	1.29	n/d	0.22	1.17	1.26	0.02	0.66	0.65	3.59	0.17
P_2O_5	0.24	0.02	0.05	0.03	0.20	0.24	0.03	0.17	0.31	0.16	0.23
Cr_2O_3	0.02	0.06	0.03	0.05	0.04	0.04	0.03	0.04	0.07	0.06	0.04
LOI	2.10	0.65	n/d	6.60	0.75	1.35	0.05	1.50	0.65	1.55	0.90
Total	98.80	100.30	98.80	99.70	98.70	98.70	98.80	98.90	99.40	99.20	98.40
Rb (ppm)	n/d	36	n/d	n/d	19	26	n/d	n/d	n/d	82	n/d
Sr	227	56	54	212	194	91	47	392	158	173	79
Y	43	n/d	28	15	23	25	29	29	33	29	40
Zr	184	50	88	41	118	95	86	100	199	151	123
Nb	19	n/d	n/d	n/d	n/d	12	n/d	n/d	12	11	n/d
Ba	59	362	n/d	78	250	202	n/d	76	80	798	53

contain varying amounts of garnet, graphite, and glaucophane; gneisses and quartzites in Unit #1 have compositional banding with different proportions of garnet, phengite, glaucophane, and, in the gneisses, clinopyroxene. The sedimentary protolith to Unit #1 host rocks was part of the leading edge of the subducting East European platform (Puchkov, 1997; Diaconescu et al., 1998; Brown and Spadea, 1999); the eclogite bodies were most likely derived from mafic intrusions associated with an early extensional event in the foreland.

Mineral compositions were analyzed using a five-spectrometer JEOL 733 electron microprobe at Stanford University; results are accurate to 1% for major elements. Representative analyses of minerals from eclogites and metasedimentary host rocks are presented in Table 3. Most garnets from eclogite boudins are almandine-rich (Alm_{54-68}, Prp_{7-29}, Gr_{8-29}, Sp_{1-4}). Garnets from host schists have much lower almandine contents (Alm_{36-41}, Prp_{28-33}, Gr_{14-19}, Sp_{13-17}); this difference probably represents contrasting bulk-rock compositions but may also reflect a later growth stage during retrograde metamorphism of the metasediments. Clinopyroxene is omphacite in composition, with jadeite component ranging from Jd_{47} to Jd_{55}. White micas are mostly phengite in composition, occurring both as a matrix phase and as inclusions within garnet in eclogite and in graphite in host schists; phengites have a consistently high Si value, ranging from 3.3 to 3.5 per formula unit (11 oxygens).

Garnet and omphacite crystallized during metamorphic stage M_{UHP}, the highest-pressure metamorphism. The UHP phases grew synchronously with the D_{UHP} deformation that probably records synsubduction deformation. On an outcrop scale, M_{UHP} garnet and pyroxene are aligned parallel to the compositional banding, termed the S_{UHP} fabric. First-stage folds are defined by compositional layering, deformed into nearly transposed tight, isoclinal folds with axial planes subparallel to the S_{UHP} foliation. Metamorphic stage M_{EF} pyroxene (eclogite-facies) is deflected around M_{UHP} garnet, giving evidence for a later high-pressure stage of pyroxene growth attending D_{EF} deformation. This later stage of folding, F_{EF}, consists of axial planes perpendicular to S_{UHP} foliation, and refolds F_{UHP} folds. Textural relations (i.e., pressure shadows and alignment in the foliation) for phengite and quartz indicate that these

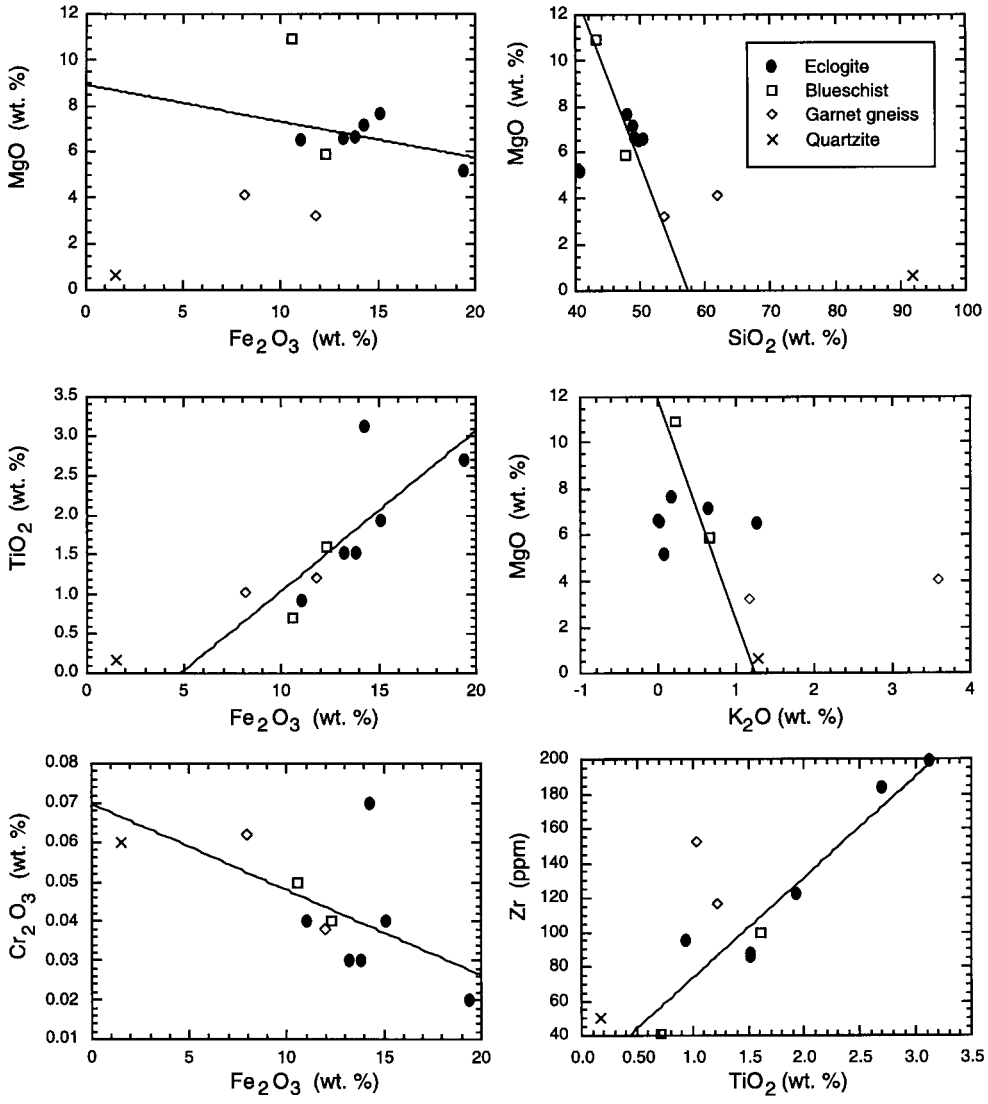

Fig. 2. Covariations of bulk-rock chemical analyses in weight percent (except for Zr in ppm) for 11 Maksyutov samples. Trend lines for parental basaltic melt evolution were approximated visually.

phases crystallized during at least two stages of metamorphism, most likely syn-M_{EF} and during the subsequent blueschist-facies recrystallization (M_{BF}).

3.3. Retrograde metamorphism and deformation

Blueschist-facies metamorphism overprints eclogite and host metasedimentary rocks of Unit #1. Hetzel et al. (1998) suggested that blueschist- and eclogite-facies metamorphism were synchronous; in contrast, we report clear evidence in the field for a late blueschist overprint on earlier eclogite-facies assemblages. The cores of many eclogite blocks and boudins contain neither blue amphibole nor lawsonite, whereas at the rims of these bodies and in the surrounding host rocks, glaucophane replaces clinopyroxene, and phengite textures show a clear blueschist-facies overprint. Localized crenulation

Table 3
Electron microprobe data for Unit #1 samples from Karayanova; MC-161 collected from Shubino

Sample no.	MC-16	MC-98	MC-161	MC-16	MC-98	MC-99	MC-161	MC-98	MC-99	MC-161
Rock type	Schist	Eclogite	Eclogite	Schist	Eclogite	Eclogite	Eclogite	Eclogite	Eclogite	Eclogite
Mineral	Phengite	Phengite	Phengite	Garnet	Garnet	Garnet	Garnet	Cpx	Cpx	Cpx
SiO_2 (wt.%)	54.145	51.128	51.151	38.143	37.483	37.910	37.550	56.405	56.049	55.610
TiO_2	0.254	0.750	0.653	0.189	0.160	0.187	0.130	0.236	0.187	0.190
AL_2O_3	29.674	24.905	24.620	22.945	21.368	22.003	21.720	11.477	11.972	10.770
Fe_2O_3 (total)	1.829	2.797	2.540	16.369	29.880	28.700	30.800	5.977	4.311	6.840
MnO	0.019	0.000	0.000	7.122	1.368	0.302	1.750	0.070	0.000	0.080
MgO	3.955	4.188	4.359	3.546	4.633	6.146	3.970	6.755	7.520	7.140
CaO	0.074	0.008	0.002	11.573	4.785	4.645	4.970	11.130	12.170	11.700
Na_2O	0.534	0.427	0.383	0.093	0.017	0.046	0.030	7.788	7.684	7.490
K_2O	9.492	10.534	10.680	0.000	0.000	0.010	0.010	0.002	0.000	0.000
Cr_2O_3	0.020	0.043	0.058	0.016	0.037	0.049	0.060	0.121	0.107	0.110
Total	99.996	94.781	94.446	99.996	99.733	99.998	100.990	99.962	100.000	99.930
	Using 11 O for phengite			*Using 12 O for garnet*				*Using 6 O for clinopyroxene*		
Si	3.398	3.446	3.459	2.959	2.974	2.963	2.964	2.012	1.990	1.991
Ti	0.012	0.038	0.033	0.011	0.010	0.011	0.008	0.006	0.005	0.007
Al	2.195	1.979	1.962	2.098	1.998	2.027	2.017	0.483	0.501	0.524
Cr	0.001	0.002	0.003	0.001	0.002	0.003	0.008	0.003	0.003	0.002
Fe (Total)	0.096	0.158	0.144	1.062	1.983	1.876	2.030	0.178	0.128	0.144
Mn	0.001	0.000	0.000	0.468	0.092	0.020	0.117	0.002	0.000	0.001
Mg	0.370	0.421	0.439	0.410	0.548	0.716	0.466	0.359	0.398	0.374
Ca	0.005	0.001	0.000	0.962	0.407	0.389	0.419	0.425	0.463	0.417
Na	0.065	0.056	0.050	0.014	0.003	0.007	0.004	0.539	0.529	0.554
K	0.760	0.906	0.921	0.000	0.000	0.001	0.000	0.000	0.000	0.000
Total	6.903	7.007	7.011	7.985	8.017	8.013	8.033	4.007	4.017	4.014
				Alm	35.35	65.44	62.51	66.95	Jd	50.10	50.50	53.96
				Pyr	14.13	18.08	23.86	15.37	Acm	5.81	2.82	3.09
				Grs	33.15	13.43	12.96	13.82	Aug	44.09	46.67	42.94
				Sps	16.13	3.04	0.67	3.86				

cleavages in blueschist are defined by the subparallel alignment of stage M_{BF} white mica, sodic amphibole, and rarer zoisite; some of those retrograded samples show evidence for three deformational events, as distinguished by cross-cutting crenulation cleavages. The third deformation event, and the corresponding F_{BF} folding is oblique to both $D_{UHP\text{-}EF}$ and $F_{UHP\text{-}EF}$ fabrics, and is developed locally as small-scale folds and the crenulation cleavage mentioned previously. Three stages of garnet growth, $M_{UHP\text{-}EF-BF}$, can be distinguished in Unit #1 eclogite and blueschist samples. First-metamorphic stage garnet is fractured and pulled apart subperpendicular to S_{UHP} in many samples, probably by the later D_{EF} deformation. A low-grade metamorphic overprint partially replaces garnet by the even later greenschist-facies assemblage (M_{GF}) chlorite, rare actinolite, and epidote; M_{BF} lawsonite is replaced in most samples by M_{GF} clinozoisite and white mica.

The Yumaguzinskaya unit may have been subjected to the same HP metamorphism, M_{BF}, as Unit #1; Yumaguzinskaya quartzites contain garnet, Na-amphibole, stilpnomelane, and white mica. The Yumaguzinskaya does not contain any mafic rocks, hence, thermobarometry is largely based on mineral assemblages in the metasedimentary rocks. Hetzel et al. (1998) associated the Yumaguzinskaya with the upper part of the eclogitic Unit #1. Although Unit #1 and the Yumaguzinakaya probably had similar protoliths (i.e., quartzofeldspathic sedimentary rocks), the mineral assemblages found in the Yumaguzinskaya are significantly different, having a much higher quartzofeldspathic component, and readily distinguished from Unit #1 metasedimentary

rocks. Unit #2 contains garnet and lawsonite pseudomorphs in M_{BF} metasomatic rocks, but probably never reached pressures greater than transitional greenschist–blueschist-facies, for Na-amphibole relics are totally lacking.

4. Structural geology

Fig. 1 presents a simplified geologic map for the Maksyutov Complex in the Karayanova area, with structural data superimposed; the cross-section shows spatial relationships between the three units. The overall structure of the complex is dominated by a NE–SW trending foliation and gentle folding of the three units about asymmetrical fold axes parallel to the dominant foliation; this large-scale fabric is probably a result of the oblique convergence and SE-directed subduction of the leading edge of the East European platform. The three units of the Maksyutov Complex must have been juxtaposed in the same subduction zone; the eclogitic Unit #1 was thrust against the Yumaguzinskaya (an inferred contact in the field) and both were later sutured against Unit #2 in a major shear zone that can be seen along the Sakmara River in the study area.

The large-scale structures are described by the stereonet data shown in Fig. 1. Poles to foliation in both Units #1 and #2 and at Station 3 demonstrate that the dominant foliation, which strikes ENE–WSW, has been folded about asymmetrical, shallowly plunging fold axes which trend southwest. The large-scale folding affects the entire complex, deforming all three units into a series of asymmetrical syn- and antiformal folds. The complex-wide folding suggests that this phase of deformation occurred during exhumation, probably after the three units had been tectonically juxtaposed; based on $^{40}Ar/^{39}Ar$ dating and apatite fission-track modelling, this folding most likely took place after about 335–315 Ma, when the three units were subjected to a common deformational and metamorphic history (Beane, 1997; Leech and Stockli, in press). Foliation data from Station 3 along the Sakmara River shows local minor variations in foliation and fold trends, but differs by no more than 20° dip. Fold axes from throughout the Karayanova area show that the trend of the main folding was refolded about axes trending SSE and correspond to a later folding episode.

5. Stable isotope geochemistry

5.1. Carbon isotopes

Carbon isotope analyses ($\delta^{13}C/^{12}C$ vs. VPDB) reveal that graphite occurring throughout the Maksyutov Complex is consistent with an origin appropriate for the sedimentary protoliths (see Leech and Ernst, 1998 for a detailed description). Graphite from Unit #1 quartzofeldspathic metasediments and mafic eclogites has a mean carbon isotope value near −28‰, retaining the original biogenic carbon signature; graphite $\delta^{13}C_{VPDB}$ from Unit #2 marble averages about −1.0‰, which corresponds to carbon isotope values characteristic of marine carbonates.

5.2. Oxygen isotopes

Oxygen isotopes may reveal the role of fluids during retrograde metamorphism (e.g., Sharp et al., 1993), and whether or not mineral assemblages crystallized under equilibrium conditions. New analytical data for the Makysutov Complex are displayed in Fig. 3, which also shows the relative partitioning of oxygen isotopes between different phases. Oxygen was extracted from mineral separates using a CO_2 laser in a BrF_5 atmosphere at the Geophysical Laboratory, Washington, DC. Gore Mountain garnet standard ($\delta^{18}O/^{16}O = 5.6$‰ vs. VSMOW) was used to calibrate the unknowns. Standard deviation for all samples was less than ±0.1‰. The bulk-rock oxygen isotope signature, $\delta^{18}O$, for Unit #1 metasedimentary rocks ranges from about +7‰ to +23‰; Unit #1 eclogite $\delta^{18}O$ values range from +8‰ to +15‰. A metabasalt and metasomatite from Unit #2 have $\delta^{18}O$ values similar to Unit #1 eclogites, +8‰ and +11‰, respectively; similarly, $\delta^{18}O$ for Unit #2 metasediments fall between +11‰ and +20‰, comparable to values of Unit #1 metasedimentary rocks. All bulk-rock samples fall within ranges typical of unaltered sediments and oceanic crust. As will be shown below, oxygen isotope values for different minerals exhibit regular partitioning behavior, and reflect the compositions of the host lithologies.

Fig. 4 shows the correlation between the $\delta^{18}O$ values of garnet and coexisting phases, demonstrating relatively systematic fractionation; such regular

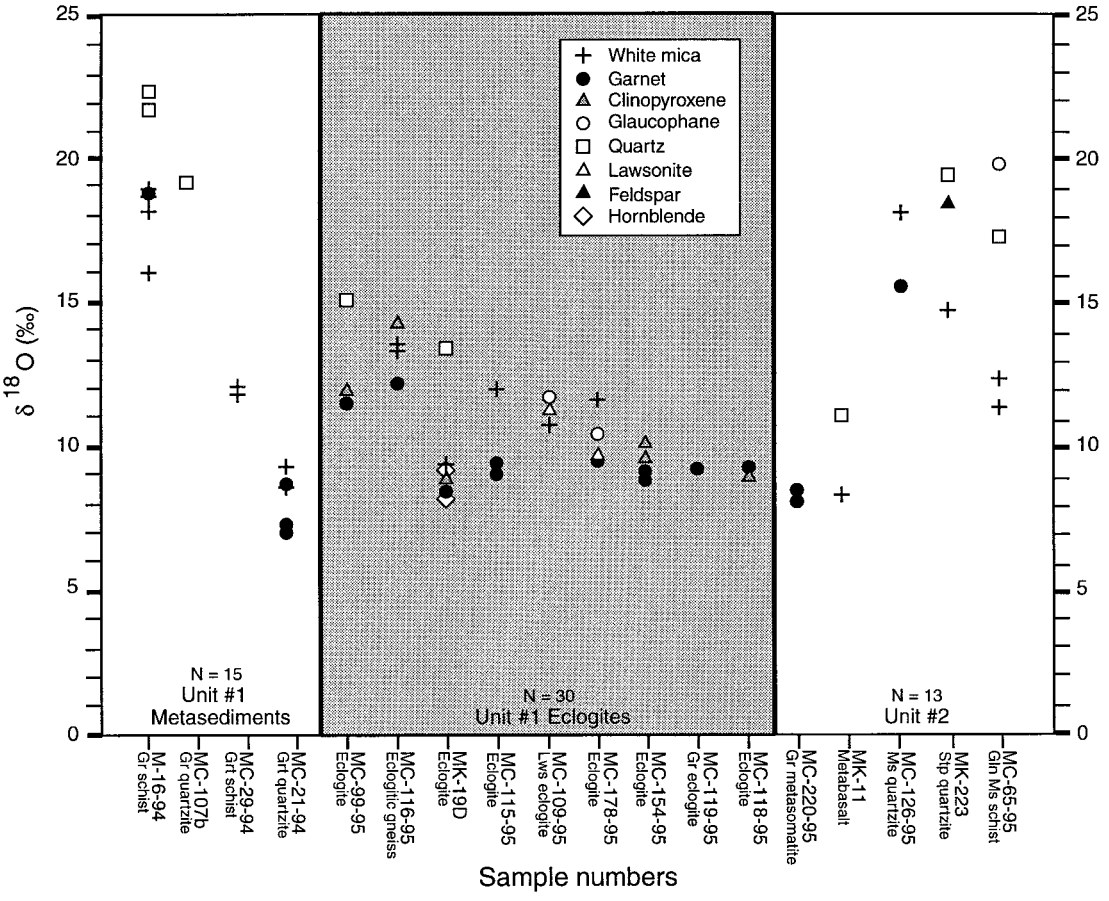

Fig. 3. Oxygen isotope data for Unit #1 metasediments and eclogites, and Unit #2 mineral separates from the Maksyutov Complex. Mineral abbreviations are after Kretz (1983).

partitioning is consistent with the hypothesis that these phases achieved isotopic equilibrium. The data imply that the different minerals crystallized synchronously during metamorphism; these data, in addition to petrographic evidence, support the conclusion that the thermobarometric calculations employing these phases are valid. Quartz is systematically enriched in ^{18}O by about 3.5‰. With the exception of white mica, garnet–clinopyroxene, garnet–clinoamphibole, and garnet–lawsonite exhibit regular, but extremely small fractionations.

Phengite, in some cases, appears to be enriched in ^{18}O by about 1–2‰ relative to coexisting garnet, but other samples lie along the equilibrium line. Textural relations of phengite with respect to eclogitic phases suggest a retrograde recrystallization of the white mica; therefore, its oxygen isotope composition may provide clues regarding the composition of the fluid attending back-reaction (Ongley et al., 1987). Retrograde phengite probably grew during the M_{EF-BF} metamorphic event, which helps constrain the timing of fluid infiltration.

5.3. Oxygen isotope geothermometry

The measured partitioning of oxygen isotopes between coexisting minerals may be utilized to evaluate the temperatures of their last equilibration, provided the phases recrystallized synchronously under conditions of chemical equilibrium (i.e., no zoning).

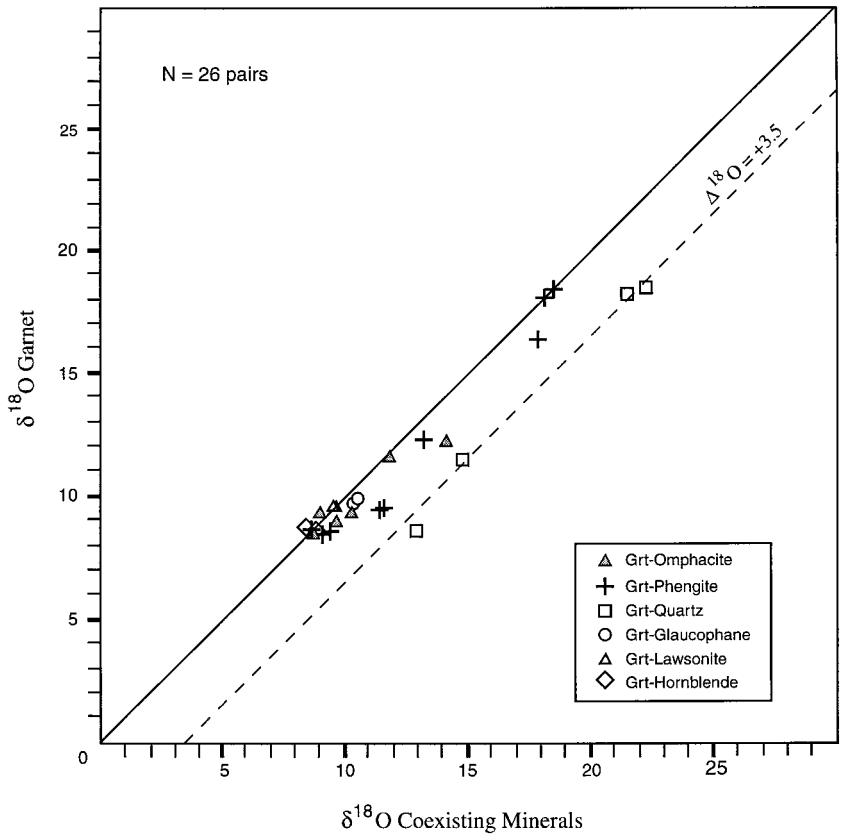

Fig. 4. Garnet and coexisting mineral-pair diagram showing that samples fall on a straight line and evidently crystallized under equilibrium conditions. The dashed line shows that quartz is systematically enriched in $\delta^{18}O$ by about 3.5‰ with respect to eclogitic phases; note also that phengite varies in $\delta^{18}O$ enrichment from 0‰ to 2‰ $\delta^{18}O$.

Furthermore, calculated temperatures are only as accurate as the experimentally determined fractionation factors for phases on which the derived *T*-values are based. We employed the fractionation data of Matthews (1994), Matthews and Schliestedt (1984), and Rosenbaum and Mattey (1995) to compute thermal conditions attending recrystallization of various phases listed in Table 4a and b. Temperatures calculated using the fractionation factor and mineral coefficients from Rosenbaum and Mattey (1995) yield values on the order of 15–20°C higher than calculations employing the data of Matthews (1994) and Matthews and Schliestedt (1984). The difference in temperature estimates for these thermometers is most likely due to the calibration of the temperature dependence of fractionation (Rumble and Yui, 1998). Rosenbaum and Mattey (1995) determined fractionation based on a higher temperature system (> 900°C) than the Maksyutov samples experienced during metamorphism, so the slightly lower temperatures calculated for quartz–garnet oxygen isotope partitioning using the Matthews and Schliestedt data record a temperature closer to the actual isotopic exchange closure temperature (Sharp, 1991). Useful mineral pairs included Qtz–Grt, Qtz–Cpx, Qtz–Pl, Qtz–Phn, and Phn–Pl. Clearly, a wide range of retrograde equilibration values are exhibited in the isotopic data. However, several tentative conclusions seem to be justified.

(1) Five quartz–garnet–omphacite equilibration values (Table 4b) from a mafic eclogite and the graphite-cuboid-bearing garnet schist range broadly

Table 4

(a) $\delta^{18}O$ values (in ‰) used for geothermometry

Sample	M-16-94	MC-99-95	MK-19D	MK-11	MK-223	MC-65-95
Rock type	Gr schist	Eclogite	Eclogite	Metabasalt	Quartzite	Gl schist
Minerals	Unit #1			Unit #2		
Phn	18.44	–	9.33	8.32	14.88	12.06
Phn	18.01	–	–	–	14.86	10.96
Phn	18.56	–	–	–	–	–
Phn	18.66	–	–	–	–	–
Phn	15.68	–	–	–	–	–
Grt	18.49	11.51	8.48	–	–	–
Grt	18.59	–	8.52	–	–	–
Cpx	11.84	11.86	8.94	–	–	–
Cpx	12.75	–	–	–	–	–
Gl	–	–	–	–	–	19.79
Gl	–	–	–	–	–	19.79
Qtz	22.09	14.81	13.32	11.14	19.57	17.16
Qtz	21.53	–	–	–	–	–
Pl	–	–	–	–	18.63	–
Hb	–	–	8.30	–	–	–
Hb	–	–	8.83	–	–	–

(b) Calculated temperatures using oxygen isotope partitioning[a]

Metamorphic stage	UHP(?)/HP			HP		LP	
	Qtz–Grt	Qtz–Grt[b]	Qtz–Cpx	Qtz–Pl	Qtz–Phn	Qtz–Phn	Phn–Pl
Unit #1							
M-16-94, Graphite schist	696	711	–	–	434	219	–
MC-99-95, Eclogite	685	704	595	–	–	–	–
MK-19D[c], Eclogite	520	535	439	–	–	350	–
Unit #2							
MC-65-95, Gl schist	–	–	–	456	–	230	–
MK-223, Quartzite	–	–	–	–	–	301	199
MK-11, Metabasalt	–	–	–	–	468	–	–
Average	678 ± 83°C			453 ± 17°C		250 ± 68°C	

[a]Temperatures calculated using fractionation factors and mineral coefficients from Matthews (1994) and Matthews and Schliestedt (1984).

[b]Values calculated from experimentally determined fractionation and coefficients from Rosenbaum and Mattey (1995).

[c]Sample not used in average temperature calculation (see text).

from 595°C to 711°C, averaging about 678 ± 83°C. These temperatures are somewhat higher, but similar to the thermobarometric values (594–637°C) arrived at by Beane et al. (1995), Lennykh et al. (1995), and Hetzel et al. (1998) for Unit #1 assemblages, based on phase equilibria and on Fe–Mg partitioning between Grt and Cpx.

Garnet records the highest closure temperature for the various mineral pairs in eclogite, from 685°C to 711°C for samples M-16-94 and MC-99-95 (Table 4b). Eclogite sample MK-19D was subjected to further isotopic exchange about 160–170°C lower than other eclogite samples, suggesting a localized fluid infiltration and re-equilibration during cooling; simi-

lar discordant temperatures between samples separated by approximately 1 m are reported for the UHP Sulu terrane (Rumble and Yui, 1998). Peak metamorphic (UHP) oxygen isotope values are probably not represented in the data inasmuch as retrograde, fluid-assisted oxygen diffusion has most likely obscured peak isotopic ratios; thermometers are known to fail to record peak temperatures in other slowly cooled high-grade metamorphic terranes (Sharp and Jenkin, 1994; Sharp et al., 1988; Eiler et al., 1992). Clinopyroxene for all eclogite samples appears to close to oxygen diffusion about 100°C lower than does garnet.

Oxygen isotope fractionation in plagioclase and phengite record two, progressively lower-temperature recrystallization events that correlate with the blueschist- and greenschist-facies metamorphic events, respectively (Table 4b).

(2) For quartz–albite and quartz–phengite pairs, three rocks — the Unit #2 metabasalt and the stilpnomelane quartzite, and the Unit #1 graphite-cuboid-bearing garnet schist — show evidence of having re-equilibrated at approximately 453 ± 17°C. Such a temperature would be appropriate for the transitional blueschist–greenschist-facies metamorphism attending shearing and the suturing of Unit #1 to Unit #2 lithotectonic units during early exhumation/decompression deep within the subduction zone.

(3) Apparent temperatures of about 250 ± 68°C provided by quartz–phengite pairs for all four metasedimentary lithologies and a phengite-bearing eclogite indicate fluid-induced metasomatism and back-reaction during late-stage uplift of the more fluid-rich, more permeable rock types.

Although these conclusions are somewhat speculative, it seems likely that the Maksyutov Complex underwent a multistage series of deformational and recrystallization/metasomatism events during its prolonged exhumation to upper crustal levels and ultimate exposure (Leech and Stockli, in press), marking the suture zone between the East European craton and central Asian microcontinental blocks (Dobretsov et al., 1996). Discordant calculated oxygen isotope temperatures are expected for slowly cooled metamorphic rocks with fluids present. Re-equilibration of $^{18}O/^{16}O$ values is further enhanced with coeval deformation at elevated pressure (Sharp, 1991; Sharp and Jenkin, 1994; Sharp et al., 1988; Eiler et al., 1992), comparable with our interpretations for the overall metamorphic and deformational evolution of the Maksyutov Complex.

6. Petrotectonic evolution

A combination of thermochronologic, fission-track data modelling, and structural, geochemical, and petrologic data constrain the evolution of the Maksyutov Complex in the context of the overall geodynamic setting of the south Ural Mountains, as described in the previous sections. Here, we present a working hypothesis for the evolution of the UHP(?) complex and adjacent lithotectonic bodies (Fig. 5).

6.1. Stage 1: Late Proterozoic to ~400 Ma

The protoliths of the Maksyutov metasedimentary rocks, part of the East European platform, are Precambrian based on radiometric dating (Dobretsov et al., 1996). Early extension along the eastern edge of the East European platform likely resulted in the shallow intrusion of mafic sills or dikes within the sedimentary section (Puchkov, 1997; Diaconescu et al., 1998; Brown and Spadea, 1999); eclogite within Unit #1 host metasedimentary rocks are likely related to these mafic intrusions. The ocean to the east of the East European platform closed and leading edge of the East European platform was subducted beneath the Magnitogorsk island arc.

6.2. Stage 2: UHP metamorphism and early exhumation to 375 Ma

U–Pb and Sm–Nd data indicate that UHP metamorphism probably occurred between about 400 and 375 Ma (Matte et al., 1993; Beane, 1997; Beane et al., 1995), but the precise timing is still uncertain. Metamorphic stage M_{UHP} minerals crystallized and the regional compositional banding and S_{UHP} foliation (along with F_{UHP} folding) developed during peak subduction-zone metamorphism. Exhumation was synconvergent and probably was accomplished by a combination of west-directed thrusting as described by Berzin et al. (1996), Echtler et al. (1996), and Brown et al. (1998), followed by normal faulting

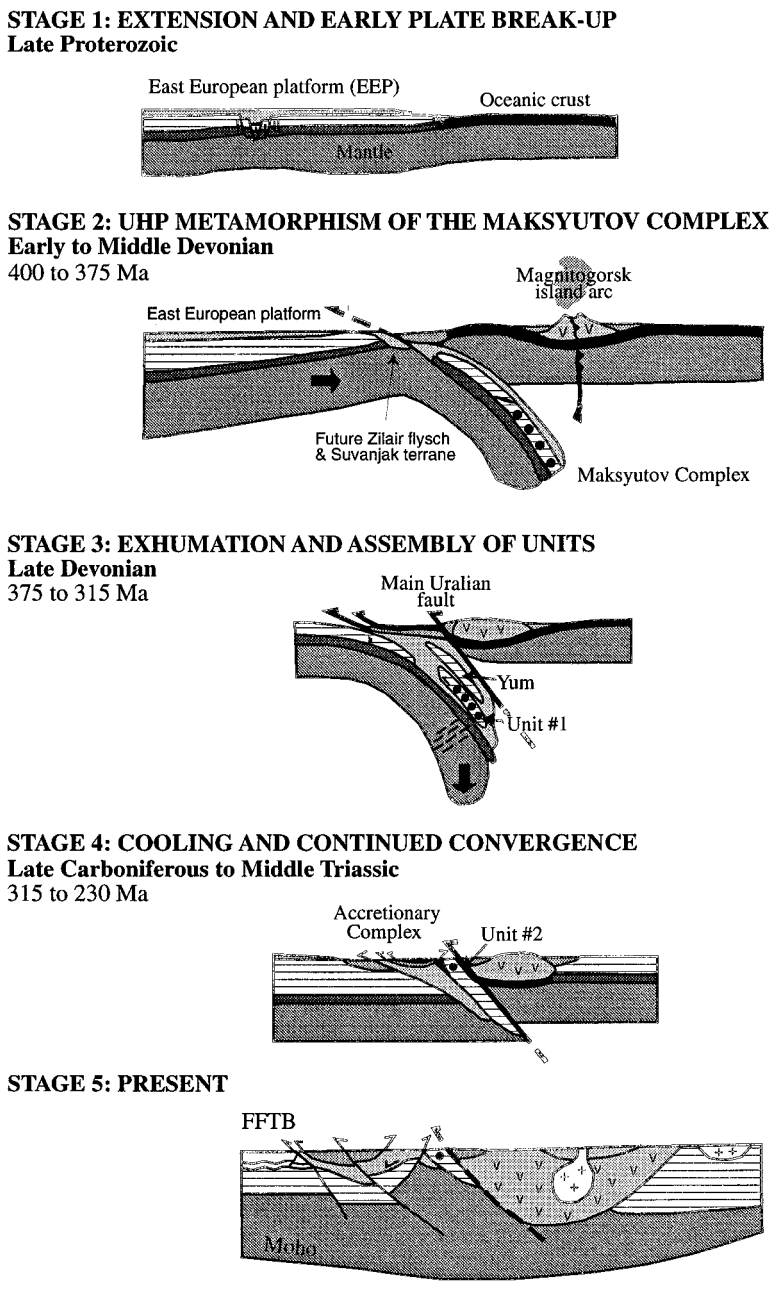

Fig. 5. Petrotectonic evolution of the Maksyutov Complex based on apatite fission track ages from Leech and Stockli (in press) and modelling from Matte (1998); Stage 5 is adapted from reflection seismic data from Brown et al. (1998). FFTB = Foreland fold-and-thrust belt.

to the east on the MUF (Fig. 5). Early stages of the exhumation probably coincided with eclogite-grade recrystallization of garnet, pyroxene, and phengite (the M_{EF} event); this recrystallization may account

for zoning in garnet and pyroxene (see Hetzel et al., 1998).

6.3. Stage 3: late exhumation and assembly of the Maksyutov Complex, 375–315 Ma

Apatite fission-track and $^{40}Ar/^{39}Ar$ data indicate that Unit #1 cooled from 350°C to 110°C between about 375 and 315 Ma (Beane, 1997; Leech and Stockli, in press). Thermal relaxation roughly coincided with the onset of the Uralian collision between the East European platform and microcontinental blocks starting in the Early Devonian (Brown et al., 1996). Thermochronologic data also indicate that the three disparate units of the Maksyutov Complex must have been tectonically juxtaposed sometime during this interval.

Between 375 and 315 Ma, both blueschist- (M_{BF}) and greenschist-facies (M_{GF}) metamorphic events and at least two stages of coeval fluid infiltration occurred as the three units of the complex were being juxtaposed within the subduction zone. Unit #1 and the Yumaguzinskaya were thrust together early in the exhumation process after about 356 Ma; the shear zone between these two amalgamated units and Unit #2 must have developed between 330 and 315 Ma, after which all three share a common history; Fig. 5 postulates that Unit #2 rocks were derived from oceanic crust in the hanging wall of the MUF, conforming to the current understanding of the structural relationship between Unit #2, the Yumaguzinskaya, and Unit #1 tectonically underlies the Yumaguzinskaya, which in turn underlies ophiolitic Unit #2. The regional-scale, southwest-trending folding that is evident in Fig. 1 most likely began during or just after the units were thrust together during continued convergence. A later south–southeast trending folding event probably took place late in this period while the rocks were still behaving ductilely.

6.4. Stage 4: cooling and continued convergence to ~ 230 Ma

After cooling to 100–80°C, fission-track modelling indicates minor reheating and, in some cases, a slowed cooling between about 315 to 230 Ma (Leech and Stockli, in press). While modelling cannot resolve this stage in detail, we interpret this reheating as the result of tectonic reburial of the Maksyutov Complex due to thrusting on the MUF during the main phase of Uralian convergence. This is consistent with the Maksyutov Complex forming the footwall to the MUF, and being overridden by west-vergent ophiolite thrust sheets (Matte et al., 1993); the fairly straight NS-trending boundaries of the complex along its western and eastern contacts probably developed as a result of this overriding thrust sheet. Apatite fission track age and track length modelling indicates a common history for footwall and hanging wall samples (i.e., only minor movement on the MUF) after the Late Carboniferous about 300 Ma (Leech and Stockli, in press).

6.5. Stage 5: cooling and final uplift

Cooling (~ 40°C) at the end of the Uralian orogeny is most simply interpreted as post-collisional erosional degradation of the mountain belt. It is possible that this stage represents post-orogenic unroofing related to extensional reactivation of the MUF, as suggested by several workers (Matte et al., 1993; Echtler and Hetzel, 1997), but thermal modelling cannot resolve significantly different histories for the footwall and hanging wall after about 300 Ma.

Fission-track data show minor but gradual reheating (~ 20°C), probably related to the transgression in which Jurassic and Cretaceous marine sediments were deposited over the MUF and the foreland fold-and-thrust belt (Brown et al., 1996; Seward et al., 1997). Final erosional denudation of the Maksyutov Complex and gradual exhumation to the present-day surface probably started in the Tertiary.

7. Conclusions

Previous thermochronological constraints on the evolution of the Maksyutov eclogite and metasedimentary host rocks have been placed in the context of the metamorphic and deformational evolution of this complex. Although general agreement exists regarding the structural evolution of the region, specific points made here augment or differ from reports by earlier workers, and are detailed to highlight their significance.

(1) Oxygen isotope data for the Maksyutov Complex indicate that garnet and clinopyroxene crystallized in isotopic equilibrium; therefore, thermobarometric calculations are valid for the metamorphic stage represented by those minerals. Whether these $P–T$ conditions represent the peak metamorphism, or simply a stage in the decompression annealing has yet to be determined. Evidence for late-stage fluid infiltration (M_{BF} and/or M_{GF}), manifested as variation in $\delta^{18}O$ values for phengite from the eclogitic Unit #1, probably reflect relatively high-pressure and later low-pressure retrograde metamorphic events. When considered with data showing a slow exhumation rate for the complex, this fluid appears to be responsible for obliterating geochemical evidence of UHP metamorphism. Coesite and diamond that may have once been present in Unit #1 rocks are now only seen as relic quartz and graphite pseudomorphs.

Oxygen isotope thermometry indicates that there were at least two stages of fluid influx during the retrograde metamorphism of the Maksytuov Complex. Calculated temperatures coincide with eclogite-facies, blueschist-facies, and greenschist-facies metamorphic and deformational events. Peak metamorphic (UHP) oxygen isotope values are probably not represented in the data; fluid-mediated oxygen diffusion has most likely obscured peak $P–T$ isotopic ratios.

(2) Blueschist-facies metamorphism was an early retrograde event that post-dated the UHP and eclogite-facies events as evidenced by rims of glaucophane on eclogite boudins, and was not coeval with the UHP or eclogite-facies metamorphism. Petrographic examination of fabrics also shows unambiguously that crystallization of glaucophane postdated the highest-pressure metamorphism.

(3) The protoliths of Unit #1 and the Yumaguzinskaya unit are similar, but have contrasting early recrystallization histories, and should be considered as different tectonic entities. Both units were metamorphosed in the same subduction zone and had a common paragenesis after about 356 Ma, but the petrology of each is distinct; in addition, the Yumaguzinskaya completely lacks eclogitic and ultramafic rocks.

(4) Our structural cross-section through the Maksyutov Complex in the Karayanova area shows two large-scale structural trends. The pervasive NE–SW penetrative fabric that affects all three units was caused by SE-directed subduction and folding of the complex during or after the units were juxtaposed early in the exhumation history. These structures were later folded about axes trending SSE, causing what may seem locally like more complex structural variation.

Fluid-enhanced retrogression of Maksyutov rocks supports earlier findings that Unit #1 rocks were subjected to UHP metamorphism; evidence for peak metamorphism is concealed by geochemical re-equilibration attending slow exhumation. Our model for the petrotectonic evolution of the Maksyutov Complex considers the most recent and comprehensive thermochronological, structural, and metamorphic data; accordingly, we believe that our petrotectonic scenario represents the most accurate picture for the overall history of the complex.

Acknowledgements

We thank Doug Rumble for his help in analyzing oxygen isotopes at the Geophysical Laboratory, and Rachel Beane for providing mineral separates. J.G. Liou, Paddy O'Brien, and one anonymous person provided helpful reviews of the manuscript. This research was supported in part by a research grant (#6075-97) from the Geological Society of America and McGee and Shell Fund grants from Stanford University both to Mary L. Leech, and an NSF grant to J.G. Liou (EAR 97-25347).

References

Beane, R.J., 1997. Petrologic evolution and geochronologic constraints for high-pressure metamorphism in the Maksyutov Complex, south Ural Mountains. PhD dissertation, Stanford Univ., Stanford, CA, 133 pp.

Beane, R.J., Liou, J.G., Coleman, R.G., Leech, M.L., 1995. Mineral assemblages and retrograde $P–T$ path for high- to ultrahigh-pressure metamorphism in the lower unit of the Maksyutov Complex, southern Ural Mountains, Russia. Isl. Arc 4, 254–266.

Berzin, R., Oncken, O., Knapp, J.H., Perez-Estaún, A., Hismatulin, T., Yunosov, N., Lipilin, A., 1996. Orogenic evolution of the Ural Mountains: results from an integrated seismic experiment. Science 274, 220–221.

Brown, D., Juhlin, C., Alvarez-Marron, J., Pérez-Estaún, A., Oslianski, A., 1998. Crustal-scale structure and evolution of an arc–continent collision zone in the southern Urals, Russia. Tectonics 17, 158–171.

Brown, D., Puchkov, V., Alvarez-Marron, J., Perez-Estaun, A., 1996. The structural architecture of the footwall to the Main Uralian Fault, southern Urals. Earth Sci. Rev. 40, 125–147.

Brown, D., Spadea, P., 1999. Processes of forearc and accretionary complex formation during arc-continent collision in the southern Ural Mountains. Geology 27, 649–652.

Chesnokov, B.V., Popov, V.A., 1965. Increasing volume of quartz grains in eclogites of the south Urals. Dokl. Akad. Nauk SSSR 162, 176–178.

Diaconescu, C.C., Knapp, J.H., Brown, L.D., Steer, D.N., Stiller, M., 1998. Precambrian Moho offset and tectonic stability of the East European platform from the URSEIS deep seismic profile. Geology 26, 211–214.

Dobretsov, N.L., Shatsky, V.S., Coleman, R.G., Lennykh, V.I., Valizer, P.M., Liou, J.G., Zhang, R., Beane, R.J., 1996. Tectonic setting and petrology of ultrahigh-pressure metamorphic rocks in the Maksutov Complex, Ural Mountains, Russia. Int. Geol. Rev. 38, 136–160.

Echtler, H.P., Hetzel, R., 1997. Main Uralian Thrust and Main Uralian Normal Fault: non-extensional Palaeozoic high-P rock exhumation, oblique collision, and normal faulting in the southern Urals. Terra Nova 9, 158–162.

Echtler, H.P., Stiller, M., Steinhoff, F., Krawczyk, C.M., Suleimanov, A., Spiridonov, V., Knapp, J., Menshikov, Y., Alvarez-Marron, J., Yunusov, N., 1996. Preserved collisional crustal structure of the Southern Urals revealed by vibroseis profiling. Science 274, 224–226.

Eiler, J.M., Baumgartner, L.P., Valley, J.W., 1992. Intercrystalline stable isotope diffusion: a fast grain boundary model. Contrib. Mineral. Petrol. 112, 543–557.

Ernst, W.G., Maruyama, S., Wallis, S., 1997. Buoyancy-driven, rapid exhumation of ultrahigh-pressure metamorphosed continental crust. Proc. Natl. Acad. Sci. 94, 9532–9537.

Hacker, B.R., Peacock, S.M., 1995. Creation, preservation, and exhumation of UHPM rocks. In: Coleman, R.G., Wang, X. (Eds.), Ultrahigh Pressure Metamorphism. Cambridge Univ. Press, New York, pp. 159–181.

Hetzel, R., Echtler, H.P., Seifert, W., Schulte, B.A., Ivanov, K.S., 1998. Subduction- and exhumation-related fabrics in the Paleozoic high-pressure–low-temperature Maksyutov Complex, Antingan area, southern Urals, Russia. Geol. Soc. Am. Bull. 110, 916–930.

Holland, T.J.B., 1980. The reaction albite = jadeite + quartz determined experimentally in the range 600–1200°C. Am. Mineral. 65, 129–134.

Kretz, R., 1983. Symbols for rock-forming minerals. Am. Mineral. 68, 277–279.

Leech, M.L., Ernst, W.G., 1998. Graphite pseudomorphs after diamond? A carbon isotope and spectroscopic study of graphite cuboids from the Maksyutov Complex, south Ural Mountains, Russia. Geochim. Cosmochim. Acta 62, 2143–2154.

Leech, M.L., Stockli, D.F., in press. Exhumation of the high- to ultrahigh-pressure Maksyutov Complex, south Ural Mountains, Russia. Tectonics.

Lennykh, V.I., Valizer, P.M., Beane, R.J., Leech, M.L., Ernst, W.G., 1995. Petrotectonic evolution of the Maksyutov Complex, south Urals, Russia: implications for ultrahigh-pressure metamorphism. Int. Geol. Rev. 37, 584–600.

Matte, P., 1998. Continental subduction and exhumation of HP rocks in Paleozoic orogenic belts: Uralides and Variscides. Geol. Foeren. Stockholm Foerh. 120, 209–222.

Matte, P., Maluski, H., Caby, R., Nicholas, A., Kepezhinkskas, P., Sobolev, S., 1993. Geodynamic model and $^{39}Ar/^{40}Ar$ dating for the generation and emplacement of the high pressure metamorphic rocks in SW Urals. C. R. Acad. Sci. Paris 317, 1667–1674, Serie II.

Matthews, A., 1994. Oxygen isotope geothermometers for metamorphic rocks. J. Metamorph. Geol. 12, 211–219.

Matthews, A., Schliestedt, M., 1984. Evolution of the blueschist and greenschist facies rocks of Sinfos, Cyclades, Greece. Contrib. Mineral. Petrol. 88, 150–163.

Mezger, K., Hanson, G.N., Bohlen, S.R., 1989. High-precision U–Pb ages of metamorphic rutile: application to the cooling history of high-grade terranes. Earth Planet. Sci. Lett. 96, 106–118.

Ongley, J.S., Basu, A.R., Kyser, T.K., 1987. Oxygen isotopes in coexisting garnets, clinopyroxenes and phlogopites of Roberts Victor eclogites: implications for petrogenesis and mantle metasomatism. Earth Planet. Sci. Lett. 83, 80–84.

Powell, R., 1985. Regression diagnostics and robust regression in geothermometer/geobarometer calibration: the garnet–clinopyroxene geothermometer revisited. J. Metamorph. Geol. 3, 231–243.

Puchkov, V.N., 1997. Structure and geodynamics of the Uralian orogen. In: Burg, J.-P., Ford, M. (Eds.), Orogeny Through Time. Geological Society Special Publication No. 121, pp. 201–236.

Rosenbaum, J.M., Mattey, D., 1995. Equilibrium garnet–calcite oxygen isotope fractionation. Geochim. Cosmochim. Acta 59, 2839–2842.

Rumble, D., Yui, T.-F., 1998. The Qinglongshan oxygen and hydrogen isotope anomaly near Donghai in Jiangsu Province, China. Geochim. Cosmochim. Acta 62, 3307–3321.

Seward, D., Perez-Estaun, A., Puchkov, V., 1997. Preliminary fission-track results from the southern Urals — Sterlitamak to Magnitogorsk. Tectonophysics 276, 281–290.

Sharp, Z.D., 1991. Determination of oxygen diffusion rates in magnetite from natural isotopic variations. Geology 19, 653–656.

Sharp, Z.D., Essene, E.J., Hunziker, J.C., 1993. Stable isotope geochemistry and phase equilibria of coesite-bearing whiteschists, Dora Maira Massif, western Alps. Contrib. Mineral. Petrol. 114, 1–12.

Sharp, Z.D., Jenkin, G.R.T., 1994. An empirical estimate of the diffusion rate of oxygen in diopside. J. Metamorph. Geol. 12, 89–97.

Sharp, Z.D., O'Neil, J.R., Essene, E.J., 1988. Oxygen isotope variations in granulite-grade iron formations: constraints on oxygen diffusion and retrograde isotopic exchange. Contrib. Mineral. Petrol. 98, 490–501.

Shatsky, V.S., Jagoutz, E., Koz'menko, O.A., 1997. Sm–Nd dating of the high-pressure metamorphism of the Maksyutov

Complex, southern Urals. Trans. (Dokl.) Russ. Acad. Sci./Earth Sci. Sect. 353, 285–288.

Sobolev, N.V., Shatsky, V.S., 1990. Diamond inclusions in garnets from metamorphic rocks. Nature 343, 742–746.

Sobolev, N.V., Shatsky, V.S., Vavilov, M.A., Goryainov, S.V., 1994. Zircon from ultra high pressure metamorphic rocks of folded regions as a unique container of inclusions of diamond, coesite and coexisting minerals. Dokl. Akad. Nauk 334, 488–492.

Webb, L.E., Hacker, B.R., Ratschbacher, L., McWilliams, M.O., Dong, S., 1999. Thermochronologic constraints on deformation and cooling history of high and ultrahigh-pressure rocks in the Qinling–Dabie orogen. Tectonics 18, 621–638.

Wilson, M., 1989. Igneous Petrogenesis. Unwin Hyman, London, UK, 466 pp.

Zalduegui, J.F.S., Scharer, U., Ibarguchi, J.I.G., Girardeau, J., 1996. Origin and evolution of the Paleozoic Cabo Ortegal ultramafic–mafic complex (NW Spain): U–Pb, Rb–Sr and Pb–Pb isotope data. Chem. Geol. 129, 281–304.

Zonenshain, L.P., Korinevsky, V.G., Kazmin, V.G., Pecherskiy, D.M., Khain, V.V., Matveyenkov, V.V., 1984. Plate tectonic model of the south Urals development. Tectonophysics 109, 95–135.

Zonenshain, L.P., Kuzmin, M.I., Natapov, L.M., 1990. Geology of the USSR: a plate tectonic synthesis. AGU Geodyn. Ser. 21, Washington, DC, 242 pp.